Dielectric breakdown field of strained silicon under hydrostatic pressure

Chiho Kim, and Rampi Ramprasad

Citation: Appl. Phys. Lett. **111**, 112904 (2017); doi: 10.1063/1.5003344
View online: http://dx.doi.org/10.1063/1.5003344
View Table of Contents: http://aip.scitation.org/toc/apl/111/11
Published by the American Institute of Physics

Dielectric breakdown field of strained silicon under hydrostatic pressure

Chiho Kim and Rampi Ramprasad[a)]
Department of Materials Science and Engineering, and Institute of Materials Science, University of Connecticut, 97 North Eagleville Road, Storrs, Connecticut 06269-3136, USA

(Received 3 May 2017; accepted 29 August 2017; published online 15 September 2017)

First-principles density functional theory calculations are used to reveal a quantitative relationship between the dielectric breakdown field and hydrostatic pressure of crystalline Si. The electronic band structure, phonon dispersion, and electron scattering rate are computed for pressures from 62.2 kbar (compressive) to -45.6 kbar (tensile) to estimate the rate of kinetic energy gain and loss for the electron. The theoretical dielectric breakdown fields are then determined using the von Hippel–Fröhlich criterion. Compressive stresses lead to a lower breakdown field, while significant increases in the dielectric breakdown field can be achieved by tensile stresses. *Published by AIP Publishing.* [http://dx.doi.org/10.1063/1.5003344]

Strain engineering in Si technology enables efficient control of hole and electron mobilities without changing the chemical composition or making structural modifications to achieve the target performance of microelectronic applications.[1–10] Under certain stress conditions, however, Si experiences a narrowing of the bandgap, leading to an increase in leakage current,[11–14] or a reduction in the dielectric breakdown field, leading to a device less endurable under high electric fields.[15,16] As applications rapidly scale down, these disadvantages become critical. A clear understanding of the relationship between strain and dielectric breakdown behaviors becomes useful.

The intrinsic dielectric breakdown field (the focus of the present work) is the highest possible electric field that a perfect material can tolerate. The theoretical limit of dielectric strength is explained in terms of electron-avalanche resulting from carrier multiplication.[17,18] Conduction electrons gain energy from the external electric field, while they lose energy due to electron-phonon scattering.[19–22] The rates of energy gain and loss are well balanced at a low electric field. Under a sufficiently large electric field, the energy of the electron increases to the threshold energy for impact ionization so that an avalanche of electrons and lattice ionization can cause irreversible damage to the material. Previous studies reported that the theoretical intrinsic dielectric breakdown field of non-strained Si is 84.2 MV/m.[20,21]

The effect of mechanical stress on the breakdown behavior has been studied from several experimental reports. Jeffery *et al.* reported that local stresses in the SiO_2 film lead to the local reductions in breakdown strength.[23] For organic insulators, such as polyethylene terephthalate, the dependence of breakdown strength on the stress appears to be more complex according to the study by Park *et al.*[24]

The goal of this study is to show the behavior of the dielectric breakdown field of Si under external pressure. We modeled perfect crystalline Si in the diamond structure and applied hydrostatic pressure in compressive and tensile regimes by varying the lattice constant. We then applied the theory of the dielectric breakdown field established by Fröhlich[16,25–27] within a recently developed first-principles framework. The electron-phonon scattering rate is derived as a function of electron energy. The gain and loss of electron energy under the electric field are calculated to deliver the dielectric breakdown field as a function of the pressure level.

The calculations were carried out using the density functional theory (DFT) with the norm conserving pseudopotential of Hartwigsen *et al.*[28] and Perdew-Burke-Ernzerhof functional[29] as implemented in the Quantum Espresso code.[30] The kinetic energy cutoff of the plane-wave was set to 544 eV. A Monkhorst-Pack $\boldsymbol{k}$-point mesh of $32 \times 32 \times 32$ (to sample the electronic states) and a $\boldsymbol{q}$-point mesh of $4 \times 4 \times 4$ (to sample the phonon states) were used to obtain converged results.[31] A reference (equilibrium) structure of Si is constructed in the diamond phase with the lattice constant, $a_0 = 5.46$ Å. Hydrostatic pressure (σ) is applied by employing *isotropic* strains defined by $\varepsilon = (a - a_0)/a_0$ in which a is the lattice constant of isotropically strained Si. The level of pressure being applied to the strained Si is determined by the Murnaghan equation of state using the lattice constant of strained Si, equilibrium lattice constant a_0, bulk modulus (883.2 kbar), and the derivative of the bulk modulus with respect to pressure (4.8).

The von Hippel–Fröhlich criterion to determine the intrinsic dielectric breakdown field is given as follows:

$$A(E,F) > B(E) \text{ for all } E \text{ in } \{CBM, E_i\}, \tag{1}$$

where $A(E, F)$ is the rate of the energy gain of an electron with energy E under electric field F and $B(E)$ is the rate of energy loss due to the scattering between the electron and phonon. The threshold energy for impact ionization, E_i, is assumed to be $CBM + E_g$, where CBM is the conduction band minimum and E_g is the bandgap calculated using the hybrid Heyd-Scuseria-Ernzerhof (HSE) exchange-correlation functional.[32] The intrinsic dielectric breakdown field is the lowest possible field for which the condition (1) is satisfied. The rate of energy loss $B(E)$ was evaluated at 300 K. The electron-phonon coupling function is computed in the linear response regime using the density functional perturbation theory (DFPT). A detailed description of the entire scheme can be found in our previous work.[20–22]

a)E-mail: rampi.ramprasad@uconn.edu

Figure 1 shows the electron and phonon band structures taken into account in the direct integration of the electron-phonon scattering probability. The indirect bandgap of Si from Γ_{15}^{v} to 0.85 X_1^c linearly decreases under hydrostatic compressive pressure, which is given as

$$E_g(\sigma) = -0.0019\sigma + 1.1829, R^2 = 0.99748, \qquad (2)$$

where E_g is the bandgap in eV and σ is the pressure in kbar (– for tensile and + for compressive stress). The behavior of the linear reduction of the bandgap by compression treated by the leading coefficient of –0.0019 eV/kbar is in good agreement with previous studies showing the pressure coefficient from –0.002 eV/kbar to –0.0013 eV/kbar.[11–14] Since we used $CBM + E_g$ as the threshold energy of impact ionization, the change in the bandgap due to hydrostatic pressure directly affects the dielectric breakdown field. Details of the relationship are described later in this letter.

The phonon dispersion is affected by hydrostatic pressure in two different ways depending on the vibrational modes. At first, transverse acoustic (TA) branches tend to soften when compressive pressure is applied. This behavior is rarely observed as other crystals generally showing softening of the phonon when tensile stress is applied. On the other hand, four other branches, i.e., the longitudinal acoustic (LA), longitudinal optic (LO), and two transverse optic (TO) modes, become rigid with compression. This dualistic behavior has been extensively studied in previous reports, and it has been shown that the change in phonon dispersion with varying lattice constants is responsible for the negative thermal expansion of Si in certain temperature windows.[33] The upper bound of the calculation of electron-phonon coupling, i.e., phonon cutoff (ω_{max}, a global maximum of the phonon frequency in cm^{-1}), is 503.2 cm^{-1} for non-strained Si. The cutoff increases with compression with a nearly linear relationship, $\omega_{max} = -0.0012\sigma^2 + 0.5624\sigma + 503.2, R^2 = 0.9999$.

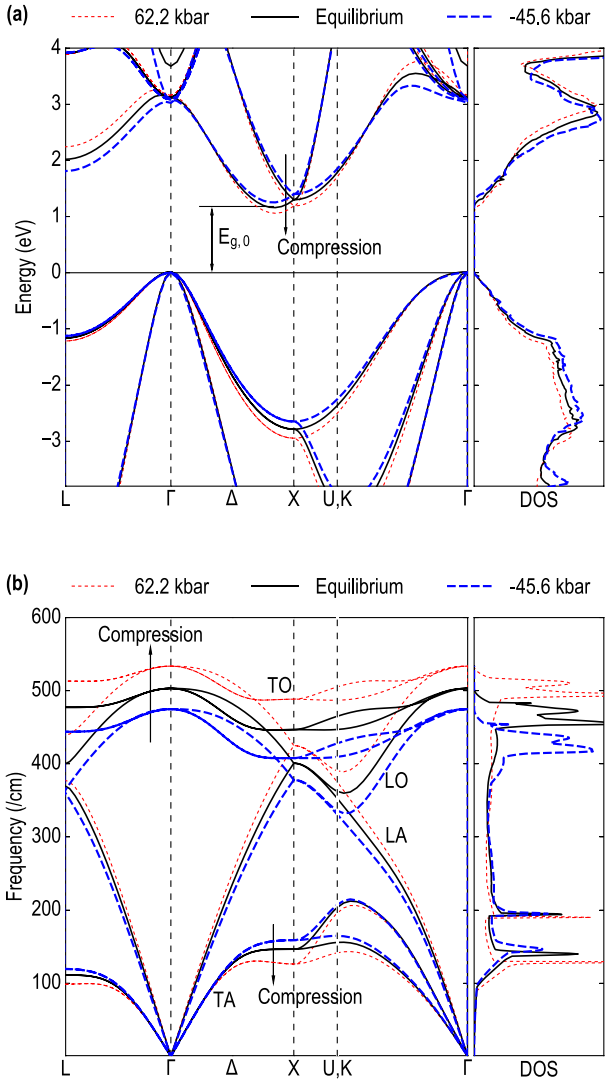

FIG. 1. Variation of the band structure and density of states (DOS) for (a) electrons and (b) phonons of Si under hydrostatic pressure. The conduction band is adjusted using the HSE level bandgap. The direction of change under compression is shown with arrows for guidance.

The computed electron-phonon scattering rate for non-strained Si at 300 K is 1.94 $\times 10^{13}$/s at the *CBM* and 1.39 $\times 10^{14}$/s at the impact ionization threshold energy corresponding to electron relaxation times 5.15 $\times 10^{-14}$ s and 7.18 $\times 10^{-15}$ s, respectively. The result agrees well with previous computation of electron-phonon scattering rates, 10^{12}/s–10^{14}/s, depending on the energy of electron, within ellipsoidal and nonparabolic energy band approximations.[34] The calculated scattering rate and threshold energy of impact ionization are listed as a function of the pressure and equivalent strain in Table I. A decrease in the bandgap under compressive stress causes suppression of the density of states (DOS) as shown in the right side panel of Fig. 1(a). A significant reduction in the electron-phonon scattering rate in spite of the increase in phonon cutoff under this compression shows that the change in impact ionization threshold energy and DOS are more dominant in electron-phonon scattering than the change in phonon cutoff.

The decrease in the scattering rate is disadvantageous to dielectric strength because scattering between the electron and phonon is the main mechanism of energy loss (cooling). In other words, the material showing a higher loss rate can withstand a higher electric field with a slow increase in the electron energy to the impact ionization threshold. The energy of the electron and applied electric field that satisfy the von Hippel-Fröhlich criterion are found at the threshold energy of impact ionization since the loss rate monotonically increases and the gain rate decreases with the energy of the electron being higher. The rates of energy gain and loss due to electron-phonon scattering are shown in Fig. 2.

TABLE I. Theoretical electron-phonon scattering rates at conduction band minimum ($1/\tau_0$) and at impact ionization threshold ($1/\tau_{E_i}$) for Si under hydrostatic pressure σ (+ for compressive and – for tensile) at 300 K. ε is the strain corresponding to the stress, and ω_{max} is the phonon cutoff frequency.

σ (kbar)	ε	E_i (eV)	ω_{max} (cm^{-1})	$1/\tau_0$ (10^{13}/s)	$1/\tau_{E_i}$ (10^{14}/s)
62.2	–0.02	1.07	533.7	1.81	1.08
28.7	–0.01	1.13	518.1	1.88	1.19
0	0	1.18	503.2	1.94	1.39
–24.6	0.01	1.21	488.8	2.02	1.67
–45.6	0.02	1.27	474.9	2.13	2.05

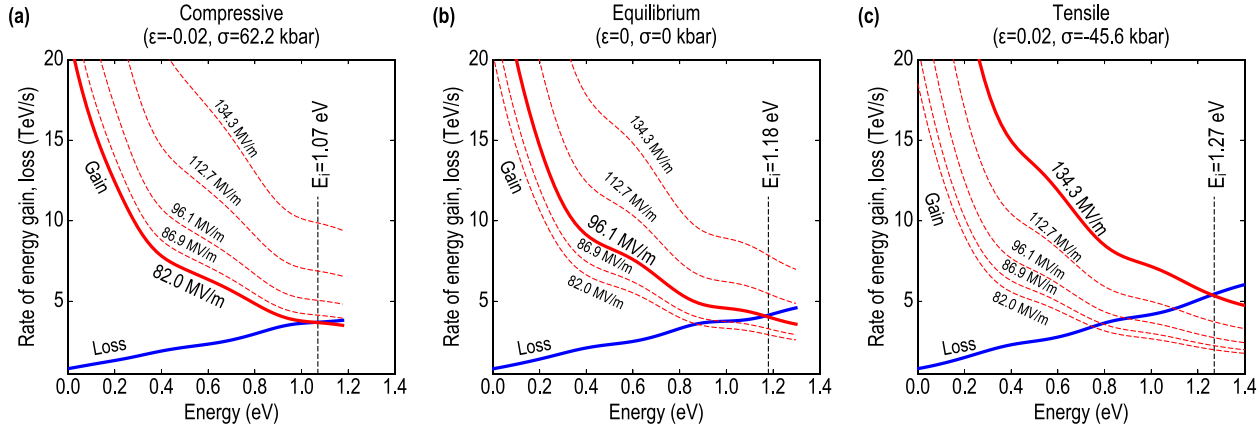

FIG. 2. Calculated rate of energy gain and loss for Si under (a) compressive stress, (b) equilibrium, and (c) tensile stress. In each panel, the energy gain rate is depicted by red curves, where a bold solid curve corresponds to the breakdown field for applied stress conditions, and dashed curves correspond to other electric fields causing dielectric breakdown of Si under stress levels listed in Table I. The threshold energy of impact ionization, E_i, is also depicted for each pressure condition.

For the case of non-strained Si, the minimum electric field for which the rate of gain is larger than the rate of loss for all energy ranges (from *CBM* to E_i) is 96.1 MV/m. This field strength is the maximum (intrinsic) dielectric breakdown field of stress-free and defect-free Si. It is hence larger than experimentally measured dielectric breakdown fields, 30 MV/m–54 MV/m.[35,36] Under compression, it is clearly seen that a relatively smaller electric field is required for electrons to reach the threshold energy for impact ionization due to significant enhancement of the gain rate and suppression of the loss rate compared to the cases of non-strained Si. As shown in Figs. 2(a) and 2(c), dielectric breakdown occurs at 82.0 MV/m and 134.3 MV/m under 62.2 kbar of compressive stress and -45.6 kbar of tensile stress, respectively.

It is worth noting that the sensitivity of the breakdown field to the stress is more significant under the tensile stress compared to compression as shown in Fig. 3. It is caused by a larger sensitivity of the energy gain rate to field strength when the applied field is larger, as $A(E, F)$ and F show a quadratic relationship.[16,20] Based on the calculated breakdown field under stress conditions ranging from 62.2 kbar to -45.6 kbar, an analytic form of the breakdown field (F_b in MV/m) can be written as a function of hydrostatic pressure in kbar,

$$F_b(\sigma) = 0.005294\sigma^2 - 0.5577\sigma + 96.86,\ R^2 = 0.9967. \quad (3)$$

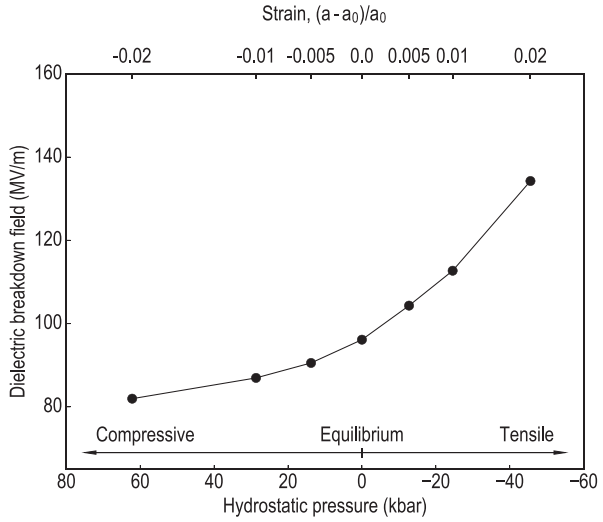

FIG. 3. Dielectric breakdown field of crystalline Si as a function of the hydrostatic pressure.

Although tensile stress can be achieved by experimental methods, e.g., growing the Si layer on substrate materials with a larger lattice constant, such as Ge and Si_xGe_{1-x},[37,38] direct comparison with current contribution is arduous because the mode of the stress applied in those experimental studies is in-plane. Further theoretical studies on the effect of in-plane stress need to be conducted.

In conclusion, we demonstrate the relationship between the dielectric breakdown field of crystalline Si and hydrostatic pressure using quantum mechanical computations. We found that the electron and phonon band structures are significantly affected by applied stress. For each stress condition, the electron-phonon scattering rate is calculated using electron bands from *CBM* to E_i and the phonon bands. Overall, tensile stresses increase the electron-phonon scattering rates, resulting in higher breakdown fields of Si. We have established the analytic form of the breakdown field as a function of hydrostatic pressure that can be used for the prediction of the breakdown field for the stress conditions ranging from 62.2 kbar to -45.6 kbar. Although the present work applies to crystalline Si with various stress levels, it is expected to provide insights into the stress dependence of dielectric strength of other insulating materials as well.

This letter is based upon the work supported by a Multidisciplinary University Research Initiative (MURI) Grant (N00014-10-1-0944) from the Office of Naval Research. Computational support was provided by the Extreme Science and Engineering Discovery Environment (XSEDE) and the National Energy Research Scientific Computing Center (NERSC). Ying Sun and Clive Bealing are acknowledged for a prior post-Quantum Espresso code development effort to compute the intrinsic dielectric breakdown field. Several useful discussions with Arun Mannodi-Kanakkithodi are gratefully acknowledged.

[1]J. Feng, X. Qian, C.-W. Huang, and J. Li, Nat. Photonics **6**, 866 (2012).
[2]N. Muralidharan, R. Carter, L. Oakes, A. P. Cohn, and C. L. Pint, Sci. Rep. **6**, 27542 (2016).
[3]W. Yang, Q.-Q. Sun, Y. Geng, L. Chen, P. Zhou, S.-J. Ding, and D. W. Zhang, Sci. Rep. **5**, 11921 (2015).
[4]A. D. Franklin, M. Luisier, S.-J. Han, G. Tulevski, C. M. Breslin, L. Gignac, M. S. Lundstrom, and W. Haensch, Nano Lett. **12**, 758 (2012).
[5]M. Du, L. Cui, Y. Cao, and A. J. Bard, J. Am. Chem. Soc. **137**, 7397 (2015).
[6]B. T. Sneed, A. P. Young, and C.-K. Tsung, Nanoscale **7**, 12248 (2015).
[7]N. Tsvetkov, Q. Lu, Y. Chen, and B. Yildiz, ACS Nano **9**, 1613 (2015).
[8]E. Parton and P. Verheyen, III-Vs Rev. **19**, 28 (2006).
[9]M. L. Lee, E. A. Fitzgerald, M. T. Bulsara, M. T. Currie, and A. Lochtefeld, J. Appl. Phys. **97**, 011101 (2005).
[10]J. Welser, J. L. Hoyt, S. Takagi, and J. F. Gibbons, in *Proceedings of 1994 IEEE International Electron Devices Meeting* (1994), pp. 373–376.
[11]X. Zhu, S. Fahy, and S. G. Louie, Phys. Rev. B **39**, 7840 (1989).
[12]T. E. Slykhouse and H. G. Drickamer, J. Phys. Chem. Solid **7**, 210 (1958).
[13]K. J. Chang, S. Froyen, and M. L. Cohen, Solid State Commun. **50**, 105 (1984).
[14]C. V. de Alvarez and M. L. Cohen, Solid State Commun. **14**, 317 (1974).
[15]I. K. Czajkowski, J. Allam, M. Silver, A. R. Adams, and M. A. Gell, in *IEE Proceedings J - Optoelectronics* (1990), pp. 79–87.
[16]H. Fröhlich, Proc. R. Soc. London, Ser. A **160**, 230 (1937).
[17]M. Sparks, D. L. Mills, R. Warren, T. Holstein, A. A. Maradudin, L. J. Sham, E. Loh, Jr., and D. F. King, Phys. Rev. B **24**, 3519 (1981).
[18]J. Y. Tang and K. Hess, J. Appl. Phys. **54**, 5139 (1983).
[19]O. J. Glembocki and F. H. Pollak, Phys. Rev. Lett. **48**, 413 (1982).
[20]Y. Sun, S. A. Boggs, and R. Ramprasad, Appl. Phys. Lett. **101**, 132906 (2012).
[21]Y. Sun, C. Bealing, S. Boggs, and R. Ramprasad, IEEE Electr. Insul. Mag. **29**, 8 (2013).
[22]C. Kim, G. Pilania, and R. Ramprasad, Chem. Mater. **28**, 1304 (2016).
[23]S. Jeffery, C. J. Sofield, and J. B. Pethica, Appl. Phys. Lett. **73**, 172 (1998).
[24]C. H. Park, M. Hara, and M. Akazaki, IEEE Trans. Electr. Insul. **EI-17**, 546 (1982).
[25]A. V. Hippel, J Appl. Phys. **8**, 815 (1937).
[26]H. Fröhlich, Nature **151**, 339 (1943).
[27]H. Fröhlich, Proc. R. Soc. London, Ser. A **188**, 521 (1947).
[28]C. Hartwigsen, S. Goedecker, and J. Hutter, Phys. Rev. B **58**, 3641 (1998).
[29]J. P. Perdew, K. Burke, and M. Ernzerhof, Phys. Rev. Lett. **77**, 3865 (1996).
[30]P. Giannozzi, S. Baroni, N. Bonini, M. Calandra, R. Car, C. Cavazzoni, D. Ceresoli, G. L. Chiarotti, M. Cococcioni, I. Dabo, A. Dal Corso, S. Fabris, G. Fratesi, S. de Gironcoli, R. Gebauer, U. Gerstmann, C. Gougoussis, A. Kokalj, M. Lazzeri, L. Martin-Samos, N. Marzari, F. Mauri, R. Mazzarello, S. Paolini, A. Pasquarello, L. Paulatto, C. Sbraccia, S. Scandolo, G. Sclauzero, A. P. Seitsonen, A. Smogunov, P. Umari, and R. M. Wentzcovitch, J. Phys.: Condens. Matter **21**, 395502 (2009).
[31]H. J. Monkhorst and J. D. Pack, Phys. Rev. B **13**, 5188 (1976).
[32]J. Heyd, G. E. Scuseria, and M. Ernzerhof, J. Chem. Phys. **118**, 8207 (2003).
[33]S. Biernacki and M. Scheffler, Phys. Rev. Lett. **63**, 290 (1989).
[34]M. Lundstrom, *Fundamentals of Carrier Transport* (Cambridge University Press, 2009).
[35]J. N. Park, K. Rose, and K. E. Mortenson, J. Appl. Phys. **38**, 5343 (1967).
[36]M. N. Yoder, IEEE Trans. Electron Devices **43**, 1633 (1996).
[37]T. Tezuka, N. Sugiyama, and S. Takagi, Appl. Phys. Lett. **79**, 1798 (2001).
[38]T. Koga, X. Sun, S. B. Cronin, and M. S. Dresselhaus, Appl. Phys. Lett. **75**, 2438 (1999).